Development 138, 1143-1152 (2011) doi:10.1242/dev.060566

Compartmentalized Notch signaling sustains epithelial mirror symmetry

Indra Wibowo[1,*], Filipe Pinto-Teixeira[1,*], Chie Satou[2], Shin-ichi Higashijima[2] and Hernán López-Schier[1,†]

SUMMARY

Bilateral symmetric tissues must interpret axial references to maintain their global architecture during growth or repair. The regeneration of hair cells in the zebrafish lateral line, for example, forms a vertical midline that bisects the neuromast epithelium into perfect mirror-symmetric plane-polarized halves. Each half contains hair cells of identical planar orientation but opposite to that of the confronting half. The establishment of bilateral symmetry in this organ is poorly understood. Here, we show that hair-cell regeneration is strongly directional along an axis perpendicular to that of epithelial planar polarity. We demonstrate compartmentalized Notch signaling in neuromasts, and show that directional regeneration depends on the development of hair-cell progenitors in polar compartments that have low Notch activity. High-resolution live cell tracking reveals a novel process of planar cell inversions whereby sibling hair cells invert positions immediately after progenitor cytokinesis, demonstrating that oriented progenitor divisions are dispensable for bilateral symmetry. Notwithstanding the invariably directional regeneration, the planar polarization of the epithelium eventually propagates symmetrically because mature hair cells move away from the midline towards the periphery of the neuromast. We conclude that a strongly anisotropic regeneration process that relies on the dynamic stabilization of progenitor identity in permissive polar compartments sustains bilateral symmetry in the lateral line.

KEY WORDS: Planar cell polarity, Cellular inversion, Bilateral symmetry, Hair cells

INTRODUCTION

The three-dimensional organization of tissues is essential for the efficient function of organs. It must also be maintained during the entire life of the individual and be recovered during organ repair because its loss can generate devastating pathologies (Wodarz and Nathke, 2007; Zallen, 2007). The pervasive planar cell polarity has emerged as an architectural property of tissues that allows investigations of the link between form and function (Axelrod, 2009; Strutt and Strutt, 2009). One group of organs that relies on planar cell polarity for coherent sensory function is the acusticolateralis system that comprises the inner ear and lateral line, the shared plane-polarized elements of which are the mechanosensory hair cells (Lewis and Davies, 2002; Rida and Chen, 2009). The planar polarization of the hair cells allows animals to detect and interpret the direction of propagation of a sound (Hudspeth, 1985). Hair cells are substantially similar in their development and physiology across species. However, although their loss in mammals is irreversible leading to permanent deafness, other vertebrates are endowed with a hair-cell regenerative capacity during their entire lives (Corwin and Cotanche, 1988; Ryals and Rubel, 1988; López-Schier, 2004; Collado et al., 2008). During organ repair, cell fate and tissue architecture are often acquired concurrently to allow functional recovery before full anatomical repair, which may be essential for organs on which animals depend for survival. In the sensory organs of the zebrafish lateral line, called neuromasts, the complete loss of hair cells triggers a rapid and precise regeneration process (Williams and Holder, 2000; López-Schier and Hudspeth, 2006; Brignull et al., 2009), during which cell fate and epithelial planar polarity are recovered progressively along three phases (Fig. 1A). Phase I commences when hair cells begin to regenerate. During this phase, the central part of the neuromast epithelium (the macula) becomes increasingly oval because it elongates along a single axis (Fig. 1C,D) (López-Schier and Hudspeth, 2006). Phase II begins when the neuromast macula expands symmetrically to regain its circular shape. During this phase epithelial planar polarity propagates laterally (Fig. 1A,E). Phases I and II last circa 30 hours each. A Phase III of homeostasis begins after around 60 hours from the onset of regeneration. During Phase I, the neuromast becomes bilaterally symmetric because a vertical midline separates the epithelium in two halves. Each half contains hair cells of identical orientation but opposite to that of the confronting half (Fig. 1D). This occurs because three processes integrate with remarkable spatiotemporal precision. First, hair cells regenerate in pairs and their soma localize adjacent to each other along the direction of epithelial planar polarity. Second, each hair cell of the pair orients opposite to its sibling within the plane of the macula. Third, all the hair cells at each side of the midline orient identically. It is not known how these processes integrate to generate bilateral symmetry. In the present study we use high-resolution live imaging in transgenic zebrafish, genetic and pharmacological perturbations of regeneration, and fluorescent sensors to address this question.

MATERIALS AND METHODS

Zebrafish strains and husbandry

Zebrafish used were maintained under standardized conditions and experiments were performed in accordance with protocols approved by the PRBB Ethical Committee of Animal Experimentation. To show different cell populations in the zebrafish neuromasts, SqET4 and SqET20 were used. For time-lapse imaging SqET4 fish were crossed to *Tg[CldB:lynGFP]* (Haas and Gilmour, 2006) to generate double transgenic

[1]Laboratory of Sensory Cell Biology & Organogenesis, Centre de Regulació Genòmica-CRG, c/Dr Aiguader 88, Barcelona 08003, Spain. [2]National Institutes of Natural Sciences, Okazaki Institute for Integrative Bioscience, Higashiyama 5-1, Myodaiji, Okazaki, Aichi 444-8787, Japan.

*These authors contributed equally to this work
†Author for correspondence (hernanls@crg.es)

Accepted 30 December 2010

larvae. The *Tg[atoh1a:tdTomato]* line was constructed from zC247L22 BAC and dTomato cDNA, and was used to analyze the expression profile of Atoh1a during regeneration. The *Tp1[bglob:hmgb1-mCherry]* line (Parsons et al., 2009) was used to report the Notch activity. *Tg[hsp70:gal4;UAS:Nicd-myc]* line, a gift from P. Chapouton (Helmholtz, Zentrum, München, Germany), was used to express a constitutively active form of Notch by heat shock during regeneration.

Neomycin treatments

Selected larvae for fixation and live imaging were treated in E3 medium containing 250 μM neomycin for 1 hour at room temperature. After treatments, larvae were washed several times using small diameter strainer to wash off residual neomycin. Larvae were allowed to recover from neomycin treatment for couple of hours before live imaging and treatments with other drugs to avoid high mortality.

DAPT and BrdU incubation

A 10 mM 5-bromo-2′-deoxyuridine (Sigma, St Louis, MO, USA) stock solution in DMSO was diluted to 10 μM in E3 medium and used to soak SqET4 larvae. Larvae were allowed to swim in this solution for 8, 24 or 48 hours, and fixed in 4% paraformaldehyde (PFA) overnight at 4°C, and then processed for immunostaining. N-[N-(3,5-Difluorophenacetyl)-L-alanyl]-S-phenylglycine t-butyl ester (DAPT, Sigma) in DMSO were used at the final concentration of 50-100 μM in E3 medium to inhibit the γ-secretase. Larvae were allowed to swim in this solution for desired time points at 28°C. As a control, larvae were treated with 1% DMSO.

Immunohistochemistry, vital labeling and fluorescent in situ hybridization

For immunohistochemistry and fluorescent in situ hybridization, larvae were fixed in 4% PFA overnight at 4°C and washed several times with 0.1% Tween-20-containing phosphate-buffered saline (0.1% PBSTw). For immunohistochemistry, larvae were immediately blocked in 10% bovine serum albumin (BSA) for at least 2 hours. For fluorescent in situ hybridization, samples were washed in gradual 25-100% PBSTw:methanol and stored at –20°C for at least 1 day. Primary antibodies and monoclonal antibodies were used at the following dilutions: mouse monoclonal antibody anti-BrdU, 1:100 (Upstate/Millipore, Billerica, MA, USA); mouse monoclonal anti-cMyc, 1:150 (NewMarkers, Fremont, CA, USA); rabbit anti-claudinB, 1:500; mouse anti-HCS1, 1:100; and rabbit anti-parvalbumin 3, 1/2000. Texas Red-labeled donkey anti-mouse and -rabbit and Cy5-labeled donkey anti-mouse and -rabbit immunoglobulin secondary antibodies (Jackson ImmunoResearch, West Grove, PA, USA) were used at 1/150. Antisense digoxigenin- and fluorescein-labeled riboprobes were synthesized according to manufacturer's instructions (Roche) by using T7/SP6/T3 RNA Polymerases. Anti-DIG and -fluorescein POD antibodies (Roche) and Tyramide Signal Amplification (TSA, PerkinElmer, Waltham, MA, USA) were used to detect antisense riboprobes. Probes used were notch3a, deltaA and atoh1a. For vital labeling of hair cells, larvae were immersed in 5 μg/ml of DiASP (Invitrogen, Carlsbad, CA, USA) in E3 medium for 2 minutes at room temperature and then washed several times to remove the excess of dye. For phalloidin staining, samples were fixed in 4% PFA overnight at 4°C then washed several times in 0.1% PBSTw and incubated in phalloidin-Alexa 568 or Alexa 488 (Invitrogen) diluted 1:20 in 0.1% PBSTw overnight at 4°C. Samples were washed several times in 0.1% PBSTw before being mounted.

Imaging and time-lapse imaging

Fluorescent images were obtained using either a Leica SP5 or SPE or Andor Spinning disk using a 40× oil immersion objective. All images were processed using ImageJ software package. For time-lapse video-microscopy, larvae were anesthetized in 0.02% tricaine (ethyl 3-aminobenzoate methanesulfonate salt, A5040, Sigma) and mounted in 1% low melting point agarose (Agarose, low melting point, A9414, Sigma) in E3 medium. Samples were imaged using either Leica SPE Leica SP5 or Andor spinning disk using a 40× oil immersion objective. Embryos were maintained at 21-25°C and *z*-stacks were collected at 2- to 10-minute intervals. Fixed samples were mounted in 0.1% PBSTw with Vectashield with DAPI (1/100, Vector Laboratories, Burlingame, CA, USA) (Faucherre et al., 2009).

Cell cycle inhibitors

Compounds for cell cycle inhibitors were used as described before (Murphy et al., 2006). Larvae were treated for the desired period with aphidicolin at 100 μM, genistein at 25 μM, nocodazole at 150 μM or colchicine at 1 mM in E3 medium supplemented with 1% DMSO.

Statistical analyses

Quantifications of BrdU-labeled cells and hair cells in whole-mounts were carried out from 10 larval-stage samples and seven neuromasts per sample. Hair cells were counted both based on GFP marker of SqET4 and apical part each hair cell as an indicator of mature hair cell. Anti-BrdU antibody was used to detect cells or hair cells incorporated BrdU. Proliferation of hair cells that appeared with or without regeneration/neomycin was calculated according to this formula: BrdU-labeled hair-cell nuclei/total number of hair cell nuclei. Total number of cells in neuromasts was calculated from DAPI staining of the nuclei. All data of BrdU incorporation are represented as percentage of the standard deviation. For experiments with the presence of DAPT, averages for controls and treated larvae were compared within each group. The same statistical analysis was used to compare between groups of controls and cell-cycle inhibitor-treated larvae. To compare the distribution of hair cell polarities in the macula of regenerating and mature neuromasts, we performed, for each condition, a one-way ANOVA that tests the null hypothesis that samples in two or more groups are drawn from the same population. For each polarity we assumed the null hypothesis that polarity distribution is homogeneous in the neuromast, comparing distributions between the ventral and dorsal halves of a neuromast and between the rostral and caudal halves.

RESULTS

Cellular heterogeneity and compartmentalization of neuromasts

Previous work has revealed that the mature neuromast is formed by the mechanosensory hair cells and by two types of supporting cells: peripheral mantle cells and central sustentacular cells (Chezar, 1930; Ghysen and Dambly-Chaudière, 2007). Lateralis hair cells regenerate in pairs and sequentially on the dorsal or ventral aspect of parallel neuromasts (Fig. 1B) (López-Schier and Hudspeth, 2006). The spatiotemporal precision of the regenerative process suggested further heterogeneity in the neuromast. We decided to interrogate cellular identity in mature organs at 7 days post fertilization (7 dpf) by characterizing transgenic lines that express the green-fluorescent protein (GFP) in the lateral line (Parinov et al., 2004; López-Schier and Hudspeth, 2006). The SqET20 line expresses the GFP in supporting cells (Hernández et al., 2007). The staining of SqET20 animals with an antibody to the pan-supporting cell marker Claudin B revealed that GFP expression was heterogeneous, showing areas with low levels of green fluorescence located at both poles of a line perpendicular to the axis of planar cell polarity of the neuromast (Fig. 1F). Strikingly, this line shifts through 90° in perpendicular neuromasts to remain perpendicular to the direction of epithelial planar polarity (Fig. 1H). The GFP^{low} areas in SqET20 also coincide with those expressing high levels of alkaline phosphatase (Fig. 1G) (Ghysen and Dambly-Chaudière, 2007; Villablanca et al., 2006). These $SqET20^{GFP\text{-}low}/AP^{+}$ areas demonstrate previously unknown compartments located at the poles of the midline of bilateral symmetry. We call them 'polar compartments'. We have previously shown that the SqET4 transgenic line expresses high levels of GFP in postmitotic hair cells, as revealed by their incorporation of the fluorescent dye DiASP, which permeates through the mechanotransduction channels (López-Schier and Hudspeth, 2006). Every DiASP(+) cell was also GFP(+), excluding the possibility that SqET4 reveals only a subset of the hair cells in the neuromast. In addition to hair cells, live imaging of SqET4 animals also

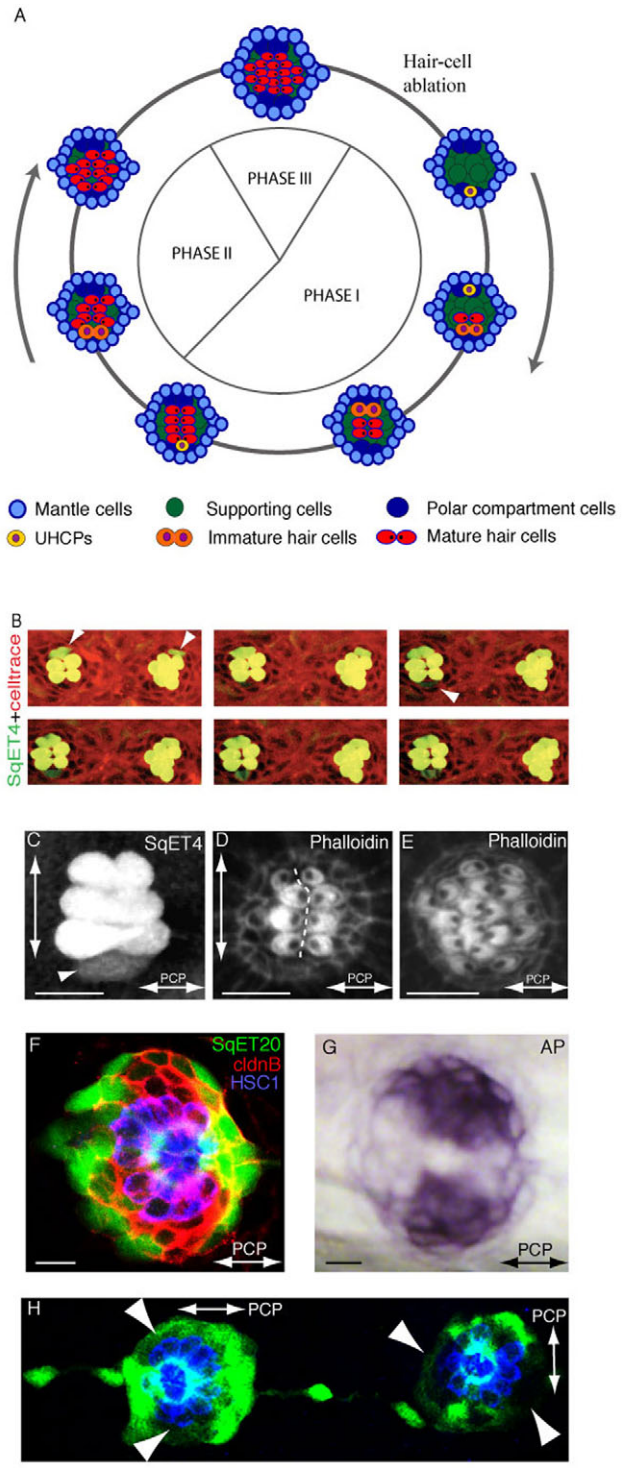

Fig. 1. Epithelial planar polarization of neuromasts. (**A**) Schematic description of the three phases of regeneration and homeostasis and the planar polarization of the neuromast epithelium (macula). Cell types are color-coded: most peripheral mantle cells (light blue), central supporting (sustentacular) cells (green), polar compartment resident cells (dark blue), UHCPs (yellow), immature hair cells (orange) and mature hair cells (red). The axis of planar polarity is evidenced by the position of the kinocilium within the mature hair cells (black dot). (**B**) Time-lapse of two adjacent parallel SqET4 neuromasts showing hair cells and their progenitors (green) and stained with Celltrace to reveal cellular boundaries (red). White arrowheads on the first panel indicate a pair of newly developed hair cells on the dorsum of both neuromasts. The white arrowhead on the third panel indicates a new ventral UHCP, which divides into two hair cells on the last panel. Hair cells develop in pairs, sequentially, and on the dorsal or ventral aspect of the neuromasts. (**C**) A regenerating SqET4 neuromast revealing six GFP-positive hair cells. A UHCP develops at the lower edge of the neuromast (arrowhead). The orthogonal axes of planar polarization (horizontal) and direction of regeneration (vertical) are indicated by double-headed arrows. (**D**) Actin staining of a regenerating neuromast, showing the orientation of four pairs of hair bundles and revealing the vertical line of bilateral symmetry (dotted white line). (**E**) Actin staining of neuromast in Phase III of regeneration showing the lateral expansion of the macula. A double-headed arrow indicates the axis of planar polarity. (**F**) A SqET20 neuromast expressing GFP (green) and stained with antibodies to Claudin-b (red), which marks all the supporting cells, and to HCS1 (blue), which highlights the hair cells. GFP^{low} compartments are located at the poles of the vertical axis of bilateral symmetry. (**G**) The GFP^{low} compartments coincide with the endogenous expression of alkaline phosphatase. In all figures, anterior is leftwards and dorsal is upwards. (**H**) A SqET20 larva expressing GFP (green) and stained with the antibody HCS1 (blue). The neuromast to the left of the image is L1 (a parallel neuromast), whereas the one on the right is L2 (a perpendicular neuromast). This image shows that the GFP^{low} compartments rotate through 90° in parallel versus perpendicular neuromasts. Arrowheads indicate polar compartments. Scale bars: 10 μm.

identified individual cells expressing lower levels of GFP (Fig. 1B,C) (López-Schier and Hudspeth, 2006). Live imaging showed that $SqET4^{GFP\text{-}low}$ cells invariably undergo a single mitosis to produce a pair of hair cells (Fig. 1B) (López-Schier and Hudspeth, 2006). $SqET4^{GFP\text{-}low}$ cells never generated cell types other than hair cells, suggesting that they are 'unipotent hair-cell progenitors' (UHCPs). From these results, we conclude that the neuromast is compartmentalized and that it contains at least five distinct cell populations: mantle cells, sustentacular cells, polar-compartment cells, transient UHCPs and the hair cells.

The mitotic division of UHCPs is essential for regeneration

It has been previously reported that mitotically active supporting cells are the main contributors to hair-cell regeneration in the zebrafish lateral line (Ma et al., 2008). However, other data suggested a role of supporting-cell transdifferentiation for the regeneration of hair cells (Hernández et al., 2007). Therefore, the relative contribution of supporting-cell proliferation versus transdifferentiation remains unknown. We decided to use the SqET4 line to resolve this issue. We started by treating 5 dpf SqET4 animals with 250 μM of neomycin for 1 hour. We have previously demonstrated that this regime eliminates the hair cells of the lateral line (López-Schier and Hudspeth, 2006). Neuromasts achieve near complete regeneration 48 hours after hair-cell ablation. After neomycin treatment, regenerating animals were left to recover in water containing the DNA synthesis marker bromo-deoxy-uridine (BrdU) (Fig. 2A). We found that 59% of the hair cells were BrdU(+) at 48 hours post treatment (hpt) (Fig. 2B,C), suggesting that proliferation and transdifferentiation could contribute to hair-cell regeneration. However, neomycin cannot kill young non-mechanoreceptive hair cells because this aminoglycoside antibiotic permeates through the mechanotranduction channels. Thus, the presence of immature neomycin-resistant hair cells in the neuromast could explain why just over half of the hair cells were BrdU(+) at 48 hpt. Another explanation for this result is that hair-cell precursors remain

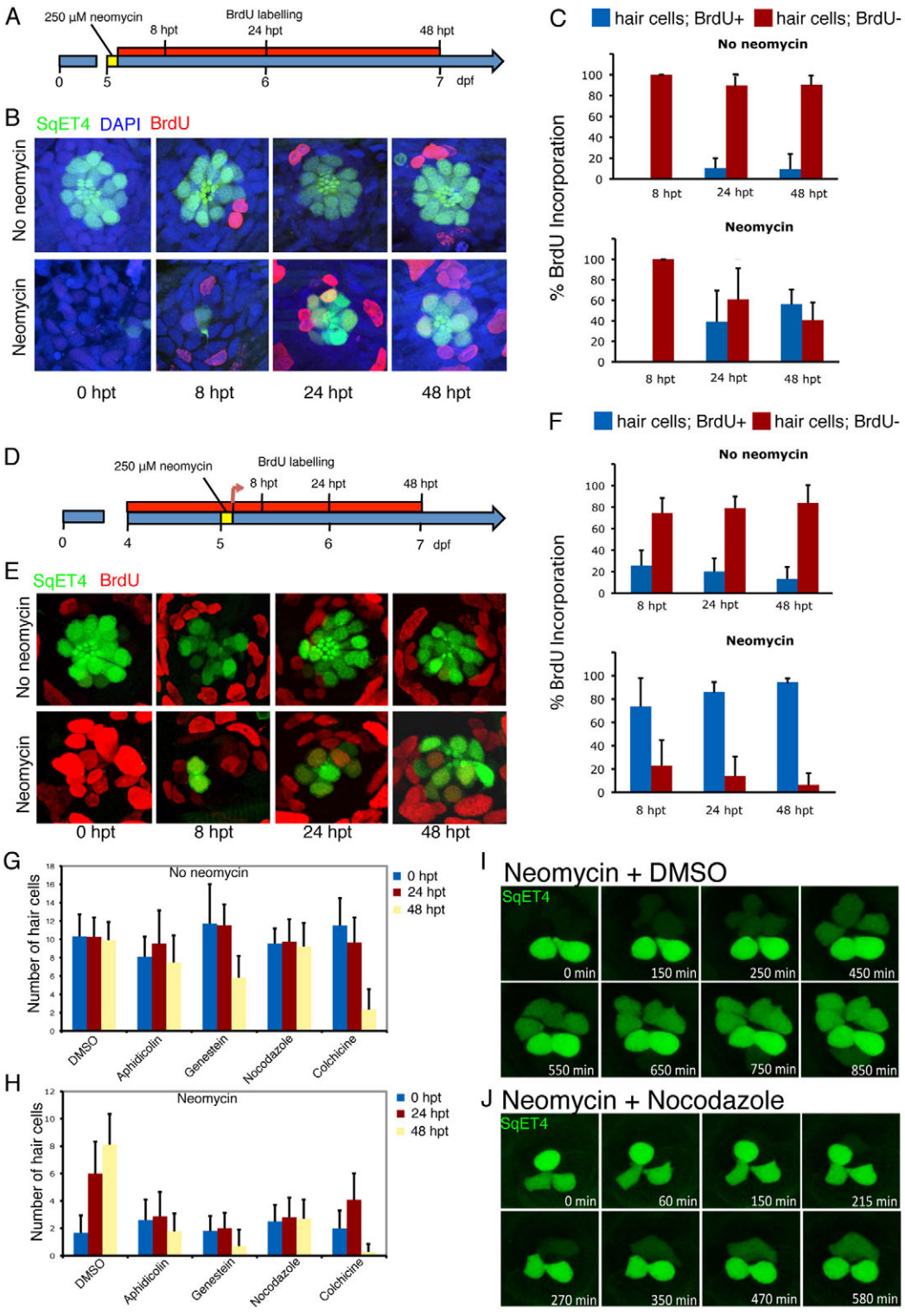

Fig. 2. See next page for legend.

arrested in a stage of the cell cycle beyond the S phase, and would progress to mitosis upon hair-cell loss without incorporating BrdU. To discriminate between these possibilities, we exposed fish to BrdU for 8 hours at 4 dpf before neomycin treatment at 5 dpf, in order to incorporate the BrdU in UHCPs and non-mechanoreceptive hair cells that may be present in the neuromast (Fig. 2D). These animals were also left to recover for 48 hours, again in the presence of BrdU. Under this condition, almost 100% of the hair cells were BrdU(+) at 48 hpt (Fig. 2E,F). This result strongly suggests that cell division is the main or the obligatory process underlying hair-cell regeneration.

To further test the extent to which mitotic activity is essential for hair-cell regeneration, we ablated hair cells in SqET4 animals with neomycin, and let them to recover in the presence of several

Fig. 2. Mitotic activity is essential for hair-cell regeneration neuromasts. (**A**) Scheme representing the experiments in which hair cells were ablated with neomycin in SqET4 transgenic zebrafish larvae at 5 dpf, and subsequently incubated continuously in BrdU for 8, 24 and 48 hours after neomycin treatment (8,24 and 48 hpt). (**B**) Confocal images of neuromasts showing hair cells in green and BrdU in red. All cell nuclei were labeled with DAPI (blue). (**C**) The mean number of GFP(+) hair cells that were BrdU(+) versus BrdU(–) in control and treated larvae at 8, 24 and 48 hpt (*n*=70 neuromasts for each timepoint). In control samples not treated with neomycin, few hair cells were labeled with BrdU at 48 hpt, whereas 59% of regenerated hair cells were BrdU(+) in neomycin-treated fish at 48 hpt. Error bars indicate s.e.m. (**D**) The experiments in which SqET4 transgenic zebrafish at 4 dpf were incubated continuously in BrdU, treated with neomycin to ablate hair cells at 5 dpf and subsequently incubated continuously in BrdU for 8, 24 and 48 hpt (results are shown in E,F). (**E**) Confocal images of neuromasts showing hair cells in green and BrdU in red. (**F**) In control samples not treated with neomycin, 74% of regenerated hair cells at 8 hpt are BrdU positive (*n*=70), compared with only 26% BrdU-positive hair cells in untreated larvae (*n*=70). By 48 hpt, 94% of regenerated hair cells are BrdU(+), compared with only 13% in untreated specimens. This finding indicates that virtually all regenerated hair cells develop from progenitors that have undergone cell division following neomycin-induced hair-cell ablation and that progenitors enter the cell cycle less than 8 hours after hair-cell death. Results are mean±s.e.m. (**G**,**H**) SqET4 transgenic larvae were incubated in several inhibitors of the cell cycle for 24 and 48 hours following neomycin treatment. The quantification shows that the number of hair cells remains relatively constant following treatments with the cell-cycle blockers aphidicolin, genistein and nocodazole in control samples (not treated with neomycin). All cell-cycle inhibitors blocked hair-cell regeneration in samples treated with neomycin. Results are mean±s.e.m. (**I**,**J**) These results were confirmed by time-lapse videomicroscopy in regenerating SqET4 control (I) and nocodazole-treated (J) larvae. Controls regenerated normally, whereas nocodazole blocked regeneration and the division of a UHCP that appears at the top of the neuromast in J.

inhibitors of the cell cycle (Fig. 2G,J). Treatments with nocodazole, aphidicolin, genistein and colchicine revealed that genistein and colchicine were the most effective suppressors of regeneration (Fig. 2H). However, control animals showed that genistein and colchicine were toxic to hair cells (Fig. 2G). Aphidicolin and nocodazole, by contrast, did not affect the viability of hair cells over a 48-hour period (Fig. 2G,J). Therefore, the nearly complete lack of hair-cell regenerates in genistein- and colchicine-treated animals may represent a compound effect of these drugs on UHCPs mitoses and hair-cell viability. This assertion is further supported by the progressive reduction of the number of hair cells at 48 hpt compared with 24 hpt in animals not treated with neomycin (Fig. 2G). Aphidicolin and nocodazole strongly suppressed hair-cell regeneration but did not completely prevent the production of GFP(+) cells. In control animals not treated with neomycin, the number of GFP(+) cells in neuromasts did not vary between 0, 24 and 48 hpt under aphidicolin and nocodazole treatment (Fig. 2G). Thus, the few GFP(+) cells present in inhibitor-treated neuromasts are likely to be hair cells that were immature at the time of neomycin treatment. Alternatively, under cell-cycle inhibition, the UHCPs that may have been already present by the time of neomycin treatment could transdifferentiate into hair cells without undergoing mitosis. To address this possibility, we directly visualized regeneration using SqET4 fish, and compared hair-cell production between control animals and those under nocodazole. Live imaging revealed that over a period of 10 hours, control animals developed 6 hair cells (Fig. 2I), whereas nocodazole-treated animals developed two hair cells and sometimes a single UHCP that could never divide or produce hair cells (Fig. 2J; see Movie 1 in the supplementary material), with the consequent arrest of regeneration. The pair of hair cells that frequently developed in nocodazole-treated fish could have been immature at the time of neomycin treatments, which may also explain why we did not achieved 100% of BrdU(+) hair cells after regeneration. We interpret these results as an indication that supporting-cell transdifferentiation does not contribute to hair-cell regeneration in the lateral line.

The orientation of UHCPs divisions is dispensable for bilateral symmetry

Regeneration in neuromasts is always progressive. Live imaging of SqET4 fish showed that UHCPs develop within or in close proximity of the dorsal and ventral polar compartments (Fig. 1B). Consequently, hair-cell regeneration is strongly directional along an axis perpendicular to that of the eventual planar polarity of the epithelium. Hair-cell siblings develop opposite planar orientation and remain adjacent to each other during Phase I. Thus, regeneration anisotropy defines the midline of bilateral planar-polarity symmetry (Fig. 1C,D). These observations led us to ask how regeneration anisotropy is controlled. Oriented cell divisions can direct growth anisotropy in epithelia (Baena-López et al., 2005; Lecuit and Le Goff, 2007). Therefore, the orientation of UHCP divisions could underlie hair-cell regeneration anisotropy and the formation of the midline of bilateral symmetry. We tested this possibility by direct visualization of 23 independent UHCPs in SqET4 animals, which showed that 14 UHCPs divided obliquely (Fig. 3A,B; see Movie 2 in the supplementary material), suggesting that the orientation of UHCP division is not directly translated into bilateral symmetry. We further validated this conclusion by directly revealing the dynamics of UHCPs using the double transgenic line *Tg[Cldnb:mGFP; SqET4]*, which express a membrane-targeted GFP in all supporting cells and a cytoplasmatic GFP in UHCPs and hair cells, allowing the evaluation of cellular behavior in vivo (Haas and Gilmour, 2006). Unexpectedly, we found that ~60% of UHCP divisions produced hair-cell pairs that rotated within the plane of the epithelium after progenitor cytokinesis (*n*=36). This is clearly demonstrated in the example shown in Fig. 3C, and Movie 3 in the supplementary material, where, 276 minutes into the time series, the immature hair-cell siblings begin to rotate within the plane of the epithelium, transiently and locally breaking the midline of mirror symmetry. This is most evident 306 minutes into the time series. A complete inversion of the hair cells precisely realigns them along the axis of planar polarity of the neuromast to reform mirror symmetry, which is evident 730 minutes into the time series. Therefore, oriented UHCP divisions are not essential for directional regeneration or bilateral symmetry.

A polar compartment is not a niche nor does it harbor stem cells

To further assess the relationship between regeneration anisotropy and bilateral symmetry, we deemed it essential to determine the mechanism that mediates the localized acquisition of the UHCP fate. We focused on the polar compartments, hypothesizing that their constituent cells either directly differentiate into UHCPs or that they represent a stem-cell niche from where UHCPs originate. An alternative possibility is that a localized stem cell population

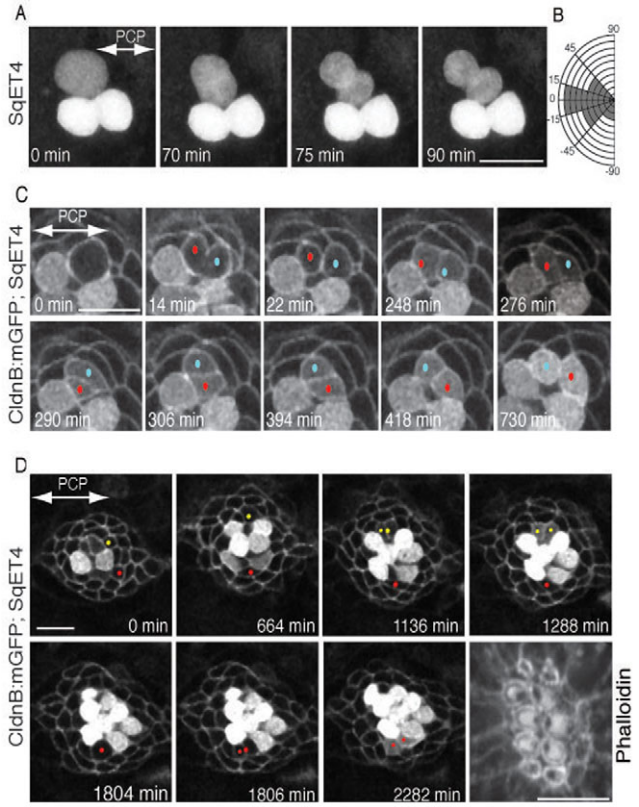

Fig. 3. Orientation of UHCP divisions and planar cell inversion. (**A**) A 90-minute series of confocal images of a regenerating SqET4 neuromast revealing two GFP-positive hair cells aligned along the axis of planar polarity (double-headed arrow). An UHCP develops at the upper edge of the neuromast. Over the next hour, this UHCP commences mitosis and divides obliquely into a pair of hair cells. (**B**) Quantification of the angle of division of UHCPs in 23 neuromasts, which indicates that the majority of UHCP divide obliquely respect to the axis of planar polarity of the epithelium. (**C**) A 12-hour series of confocal images of a regenerating neuromast of a double-transgenic *Tg[Cldnb:mGFP;SqET4]* larva revealing two GFP-positive hair cells at the lower aspect of the image, and a UHCP at the top. At 14 minutes into the time-series, this UHCP divides into two hair cells, each identified with a dot (red and blue). At 264 minutes after cytokinesis (276′), the sibling hair cells begin to rotate around their contact point within the plane of the epithelium, which locally breaks the line of mirror symmetry (this is most evident at 306 minutes into the time series). A complete inversion of the hair-cell pair eventually reforms the line of mirror symmetry and precise realigns the cells along the axis of planar polarity of the neuromast (double-headed arrow in the first panel). (**D**) A 44-hour series of confocal images of a regenerating neuromast of a double-transgenic Tg[Cldnb:mGFP;SqET4] larva reveals plasma-membrane GFP-positive supporting cells and cytoplasmatic GFP-positive hair cells and UHCPs. Two prospective UHCPs were identified retrospectively by playing the time series backwards, and each labeled with either a red or yellow dot. Their position was followed over time, showing that prospective UHCPs moved into the dorsal (yellow) and ventral (red) polar compartments, where they became UHCPs (weak cytoplasmatic GPF). Each UHCP eventually divided into a pair of hair cells. The last panel of the image is an actin staining, showing the resulting planar polarization of the epithelium. The axis of planar polarity of the neuromast is indicated by a double-headed arrow in the first panel. Scale bars: 10 μm.

does not exist in the neuromast. An extension of this proposition is that the polar compartment is not a niche. We tested these hypotheses by continuous imaging of regenerating neuromasts at single-cell resolution for periods ranging between 32 and 48 hours using *Tg[Cldnb:mGFP; SqET4]* double transgenic fish. We evaluated cellular behavior before and after UHCP development, and directly tracked cellular movement, proliferation and fate acquisition in vivo. Prospective UHCPs were identified retrospectively by playing the time series backwards, and each labeled with a colored dot. Cells were followed forward over time in all 10 successful long-term recordings, which consistently showed that although most neuromast cells do not change their relative position, some individual supporting cells relocated to the areas defined by the polar compartments, where they subsequently became UHCPs (Fig. 3D; see Movie 4 in the supplementary material). This result shows that prospective UHCPs originate elsewhere in the neuromast. It also indicates that the polar compartments are not stem-cell niches. On the contrary, these compartments represent an environment that opposes a niche to permit the differentiation of UHCPs.

Notch signaling controls the production of hair-cell progenitors

Notch signaling is universally required for hair-cell development in vertebrates (Eddison et al., 2000; Haddon et al., 1998; Lanford et al., 1999; Ma et al., 2008). To understand the mechanism that underlies UHCP-fate acquisition, we used as tools two complementary approaches that combined live imaging with genetic and pharmacological alterations of Notch signaling. First, we expressed a constitutively active from of Notch (N^{ICD}) by heat-shock during regeneration using triple transgenics *Tg[hs70p:Gal4; UAS:N^{ICD}-Myc; SqET4]*, which blocked the production of UHCPs and hair cells (Fig. 4A). In a converse experiment, we abrogated Notch activity by treating SqET4 fish with the γ-secretase inhibitor DAPT, which generated ectopic and supernumerary UHCPs and hair cells (Fig. 4A,B) (Ma et al., 2008). These results suggest that a majority of supporting cells can become UHCPs upon loss of Notch signaling. To test this possibility directly, we continuously imaged regenerating *Tg[Cldnb:mGFP; SqET4]* fish under DAPT treatment and found that UHCPs developed ectopically and in excess (Fig. 4B,C; see Movie 5 in the supplementary material). Importantly, loss of Notch broke directional regeneration and led to planar polarity defects (Fig. 4B).

Compartmentalized Notch signaling controls regeneration anisotropy

Our previous results clearly show that Notch signaling controls the differentiation of UHCPs, but do not explain why UHCPs are produced within the polar compartments. The spatiotemporal development of UHCPs shadows the expression pattern of the hair-cell determination factors DeltaA and Atoh1a (Ma et al., 2008), suggesting that these genes are first expressed by the UHCPs. To test this possibility directly, we imaged hair-cell regeneration in a double-transgenic line expressing a red-fluorescent protein under the transcriptional control of the Atoh1a promoter, combined with the UHCPs marker SqET4. Live imaging of *Tg[Atoh1a:TdTomato; SqET4]* fish showed that Atoh1a is expressed at low levels in some supporting cells that we regard as prospective progenitors (see below), and is strongly upregulated by the UHCPs at the dorsal or ventral part of parallel neuromasts, where the polar compartments are located (Fig. 4D; see Movie 6 in the supplementary material). Cell expressing high levels of Atoh1a:TdTomato were also GFP(+) and divided to produce a pair of hair cells, indicating that $Atoh1^{strong}$ cells are UHCPs. Atoh1 is a well-characterized negative transcriptional target of Notch (Itoh and Chitnis, 2001), suggesting

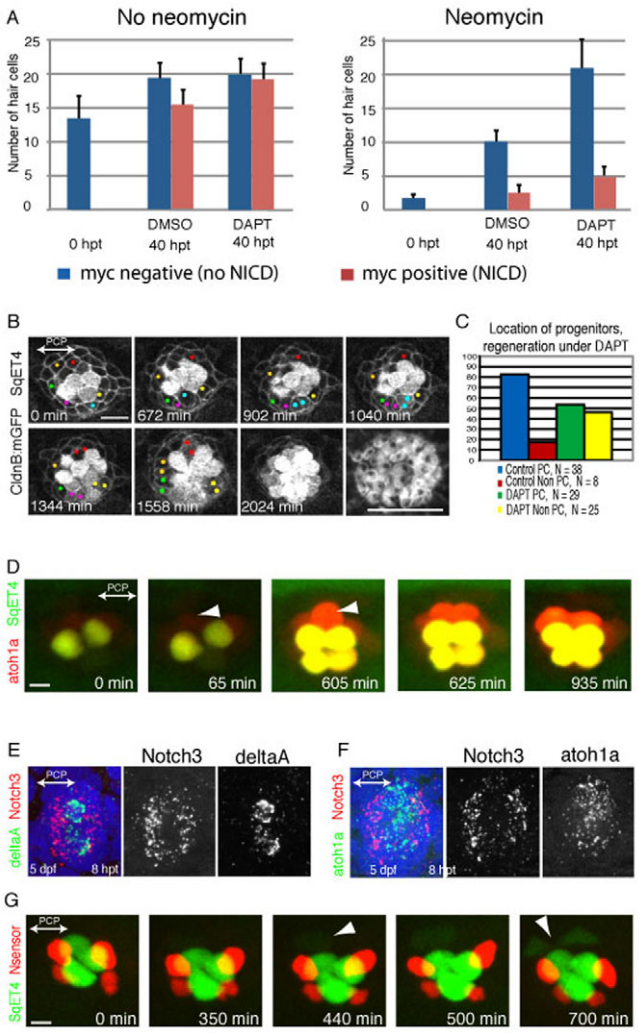

Fig. 4. UHCP develop in polar compartments. (**A**) Quantification of the average number of hair cells in samples that were treated with neomycin (right) or that were not treated (left), and later exposed to DMSO or DAPT, and that expressed (red) or did not express (blue) a constitutively active form of Notch. It shows that DAPT induces the overproduction of hair cells, and this effect is suppressed by Notch activity. Results are mean±s.e.m. (**B**) A 34-hour time series of a regenerating *Tg[Cldnb:mGFP; SqET4]* neuromast treated with DAPT. UHCPs were identified retrospectively by playing the time series backwards, and labeled with colored dots. UHCPs develop in excess, producing pairs of hair cells ectopically. Actin staining shows the resulting defective planar polarization (last panel). (**C**) A graph showing the position of UHCPs relative to the polar compartments in control and DAPT-treated neuromasts during regeneration. More than 80% of UHCPs develop within the polar compartments in controls, compared with just over 50% in DAPT-treated samples (*n*=25). Results are mean±s.e.m. (**D**) Time series of a *Tg[Atoh1a:TdTomato; SqET4]* double-transgenic neuromast revealing GFP-positive UHCPs and hair cells (green), and Atoh1a-expressing cells (red). It shows the temporal gene-expression hierarchy. Arrowheads indicate UHCPs. (**E**,**F**) Fluorescent whole-mount in situ hybridizations of regenerating neuromasts, revealing Notch3 (red) and DeltaA (green) (E), and Notch3 (red) and Atoh1a (green) (F). Cell nuclei are in blue. Notch3 is never expressed by the DeltaA(+) or Atoh1a(+) cells, and was absent from the polar compartments. (**G**) A 700-minute live imaging of a double-transgenic SqET4 (green) neuromast expressing a red-fluorescent Notch sensor (red). Notch signaling occurs outside the polar compartments. Arrowheads indicate UHCPs.

that either Notch activity is low in the polar compartments, or that prospective progenitors become refractory to Notch signaling. Our previous live imaging analyses of regenerating *Tg[SqET4; Cldnb:mGFP]* fish under DAPT treatment indicated that the majority of supporting cells can become UHCPs upon loss of Notch signaling. These results, together with the evidence that loss of Notch signaling expands Atoh1a expression (Itoh and Chitnis, 2001; Ma et al., 2008), indicate that supporting cells are not intrinsically refractory to Notch. Thus, some supporting cells are able to express the UHCP fate within the permissive environment of the polar compartments where Notch activity may be low or absent. Notch3 is the main receptor expressed in neuromasts and is dynamically regulated during hair-cell regeneration (Ma et al., 2008). To reveal the spatial expression pattern of Notch3, we used whole-mount fluorescent two-color in situ hybridization in combination with the UHCP markers Atoh1a and DeltaA. We found that Notch3 is strongly enriched in neuromast areas complementary to those expressing DeltaA and Atoh1a (Fig. 4E,F). Importantly, Notch3 was absent from the areas representing the polar compartments. To assess Notch signaling status directly in neuromasts, we used a validated red-fluorescent Notch sensor in combination with SqET4 (Parsons et al., 2009). Live imaging of neuromasts expressing this combination of markers showed that Notch activation occurs outside the polar compartments (Fig. 4G). Collectively, these results indicate that Notch activity governs hair-cell regeneration anisotropy by preventing supporting cells from becoming progenitors outside the polar compartments.

Centrifugal movement of hair cells propagates planar polarity horizontally

During phase II of regeneration, the neuromast macula loses its oval shape to become rounder because the hair-cell population expands in a direction perpendicular to that of regeneration. Consequently, planar polarity propagates laterally across the epithelium (López-Schier and Hudspeth, 2006) (Fig. 1A,E). This may occur because hair cells move away from the midline, or because UHCPs begin to appear ectopically in the neuromast during this phase. To discriminate between these possibilities, we divided the neuromast by a Cartesian grid and gave positional values to the hair bundle of each hair cell to calculate the spatial distribution of each polarity (Fig. 5A-D). This analysis showed that nearly 100% of the hair cells of each orientation were placed in separate compartments at either side of the vertical midline during phase I (Fig. 5A,B). A strongly biased distribution of polarities is maintained at either side of a vertical midline bisecting fully regenerated neuromasts (Fig. 5C,D). Importantly, comparison of polarity distributions across a horizontal midline showed distributions of 52/48% in each compartment, indicating no polarity distribution bias between the dorsal and ventral halves of parallel neuromasts (Fig. 5D). These observations support the possibility that the macula expands horizontally by a centrifugal movement of hair cells. During hair-cell development, there is a temporal hierarchy of gene expression along which cells transition as follows: SqET4^{-}/Atoh1a^{weak+} (prospective UHCPs) → SqET4^{+}/Atoh1a$^{strong+}$ (UHCPs and immature hair cells) → SqET4^{+}/Atoh1a^{-} (mature hair cells) (Fig. 5E). We evaluated the expression of these markers in fully regenerated neuromasts using triple transgenics *Tg[atoh1a:TdTomato; SqET4; Cldnb:mGFP]* and found that the oldest hair cells (SqET4^{+}/Atoh1a^{-}) were located at the periphery of the neuromast furthest from the midline of bilateral symmetry, whereas the youngest pairs (SqET4^{+}/Atoh1a$^{strong+}$) were central and described the typical direction of regeneration that connects the dorsal and ventral polar compartments (*n*=9) (Fig. 5F).

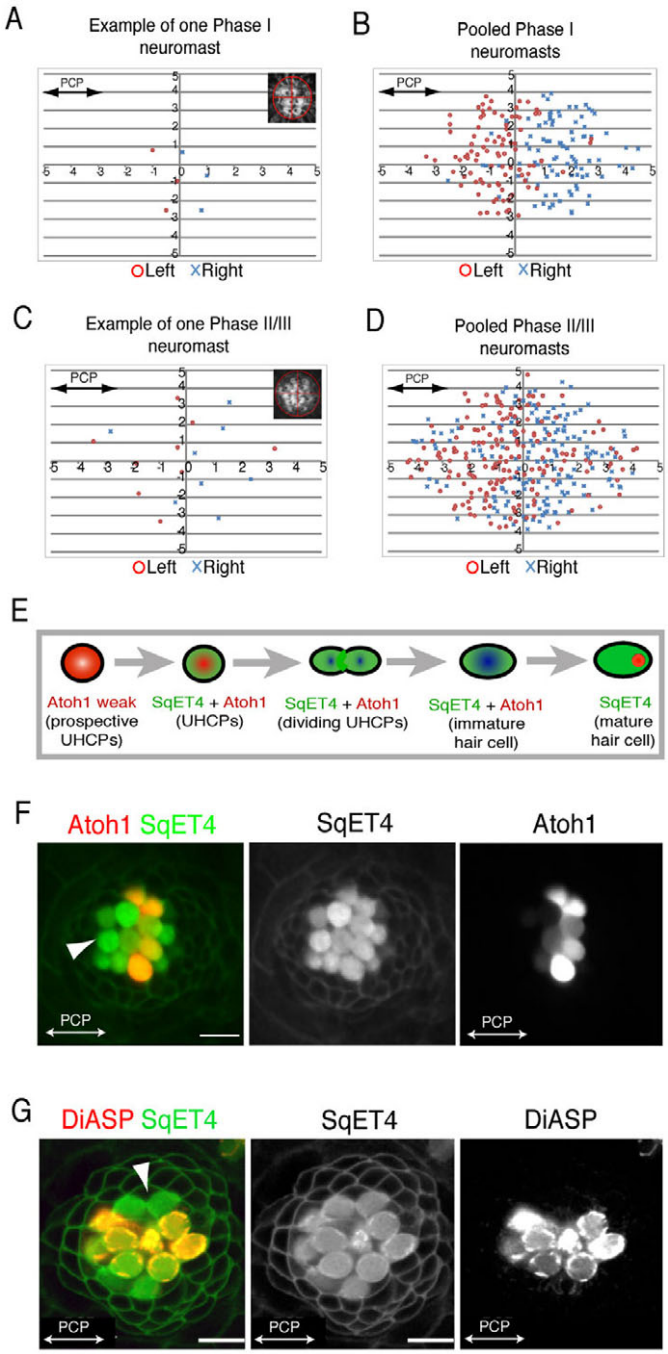

Fig. 5. Local and global planar polarization of the neuromast epithelium. (**A-D**) Hair-cell planar polarity distribution in regenerating and mature neuromasts. Positional values of each polarity are plotted in a Cartesian plane. (A,B) Example of one neuromast (A) and 20 pooled neuromasts (B) in Phase I. (C,D) Example of one neuromast (C) and 22 pooled neuromasts (D) in Phase II/III. (**E**) Schematic transition of marker gene-expression in prospective UHCPs [weakly Atoh1a+ (pink)], UHCPs, immature and young hair cells [co-expressing SqET4 and Atoh1a (green/red)], and mature hair cells [exclusively SqET4+ (green)]. (**F**) A *Tg[Atoh1a:TdTomato; SqET4]* neuromast exemplifies this transition [GFP(+) UHCPs and hair cells (green) and Atoh1a(+) cells (red)]. The white arrowhead indicates mature hair cells on the rostral part of this parallel neuromast. (**G**) DiASP incorporation into hair cells of *Tg[Cldnb:mGFP; SqET4]* neuromast, showing the exclusion of mature hair cells from the polar compartments. The white arrowhead indicates immature hair cells on the dorsal part of this parallel neuromast.

DiASP incorporation experiments that discriminate between immature and mature (mechanotransducing) hair cells revealed that older cells described a line perpendicular to that of the direction of regeneration (Fig. 5G). Importantly, DiASP(+) cells were always excluded from the polar compartments where the UHCPs and immature hair cells are preferentially located (Fig. 5G). These results, together with the scarcity of UHCPs outside the polar compartments (Fig. 3D, Fig. 4C), indicate that the horizontal expansion of planar polarity is not caused by the ectopic development of UHCPs, and that it is likely to occur because older hair cells that maintain their original orientation move away from the midline of the neuromast towards its periphery.

DISCUSSION

Hair-cell regeneration anisotropy and bilateral symmetry are functionally linked

During the initial phase of hair-cell regeneration in the zebrafish lateral line, a vertical midline bisects the neuromast epithelium into perfect mirror-symmetric plane-polarized halves. Each half contains hair cells of identical planar orientation but opposite to that of the confronting half. Hair-cell regeneration is strongly directional along the axis of bilateral symmetry. Our results explain the reason behind this reproducible behavior. It occurs because the development of UHCPs is spatially restricted to the dorsal or ventral polar compartments. The division of UHCPs into two hair cells, coupled with a consistent opposite planar orientation of the hair-cell siblings along a single axis, eventually defines the midline of mirror symmetry. Live imaging demonstrates that oriented progenitor divisions are not essential for regeneration anisotropy. Therefore, bilateral symmetry is sustained by a strongly anisotropic regeneration process that relies on the stabilization of progenitor identity in permissive polar compartments. An additional important aspect of our results is that they conclusively demonstrate that the SqET4 transgenic line highlights bona fide hair-cell progenitors, the proliferation of which is essential for hair-cell regeneration in the lateral line. This conclusion is further supported by a recent publication reporting that the promoter element of the *atp2b1a* gene is responsible for the expression pattern of the GFP in the SqET4 transgenic line, and that a morpholino-mediated knockdown of *atp2b1a* negatively affected the division of the hair-cell progenitors (Go et al., 2010).

Regeneration anisotropy is not due to a localized stem-cell population

One explanation for the compartmentalized acquisition of UHCP identity is that the polar compartments are stem cell niches. Live imaging indicates that this is unlikely because prospective UHCPs originate elsewhere in the neuromast. Thus, the polar compartments appear to be a permissive environment for the acquisition of UHCP identity by supporting cells. One possibility is that an intrinsic cell-fate determinant instructs some supporting cells to become UHCPs, and that intercellular signals prevent these cells from fully executing their differentiation until they reach a polar compartment. Previous results suggest that the source of hair-cell progenitors are the Sox2(+) cells that reside basally in the neuromast epithelium (Hernández et al., 2007). The observation that in the mouse, chick and zebrafish ears, the combinatorial activity of Sox2 and Notch control the development of pro-sensory patches, from where hair cells will eventually develop supports this proposition (Daudet et al., 2009; Millimaki et al., 2010). Future experiments involving loss- and gain-of-function of Sox2 in the lateral line will allow this possibility to be tested directly.

Regeneration anisotropy depends on compartmentalized Notch signaling

What controls the spatiotemporal development of UHCP? When Notch activity was blocked in the whole organ by DAPT treatments, directional regeneration was broken, indicating that compartmentalized Notch signaling prevents the ectopic development of hair-cell progenitors. Using fluorescent sensors and live imaging, we demonstrate that the polar compartments have low levels of Notch signaling. Because the localization of the polar compartments does not change over time, a consequence of UHCP development within them is the anisotropic regeneration of the hair cells. We have observed that hair-cell regeneration is always progressive. Live imaging of SqET4 fish showed that UHCP development alternate between the dorsal and ventral aspects of the neuromast. One explanation for the progressive development of UHCPs is that Ahtoh1a in the UHCPs and in young hair cells activates the expression of Notch ligands cell-autonomously. In turn, lateral inhibition originating from these cells would prevent the surrounding supporting cells from becoming new progenitors until hair cells have matured and lost Atoh1a expression. This would decrease the number of cells expressing Notch ligands, allowing the organ to re-set and develop new UHCPs. It will be necessary to define the identity of the relevant Notch ligands and to manipulate their activity in a cell-specific manner to test this hypothesis.

The origin of axial references remains unknown

One outstanding question is the origin of axial references and whether they rely on long-range signals. If this were the case, disruptions of regeneration anisotropy should not affect epithelial planar polarity because hair cells would be properly oriented regardless of their position in the epithelium. It follows that disruptions of Notch that break regeneration anisotropy should not cause planar-polarity defects in the epithelium. However, loss of Notch signaling randomizes hair-cell orientation, arguing against a role of long-range cues in polarizing the epithelium. However, we cannot currently rule out the possibility that Notch signaling directly controls the establishment of axial references for planar polarity by affecting the expression, transport or interpretation of long-range polarizing cues. Future experiments using iterative cycles of hair-cell ablation and regeneration, with an intervening blockade of Notch signaling, may be able to provide evidence for or against a role of Notch in the control of polarizing cues. An alternative possibility that could reconcile the effect of loss of Notch with a role of long-range polarization is that Notch signaling controls the positioning of the organelle that defines planar polarity in this tissue, the kinocilium of the hair cell. Under this scenario, loss of Notch would not allow kinocilia to respond to external polarizing cues. However, we believe that this is not likely because loss of Notch signaling in the mouse and the zebrafish ears produce normally polarized hair cells, which align in similar directions to their neighbors (Haddon et al., 1998; Lewis and Davies, 2002). In addition, a disruption of the internal machinery for planar polarity in the cell by loss of Notch should generate some hair cells with centrally located kinocilia, a phenotype that we have never observed. With our current knowledge, the most likely explanation for the planar polarity defects in neuromasts lacking Notch signaling is that supernumerary hair cells produce mechanical disturbances or packaging defects. Thus, a role for long-range polarizing signals at the origin of axial references remains a possibility.

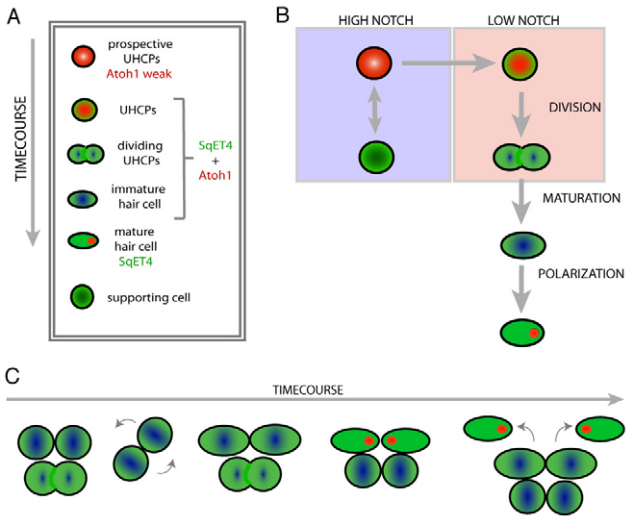

Fig. 6. Model of epithelial planar polarization in the neuromast. (**A**) Scheme of the different cell types or cell status in the neuromast. Cellular identities are color coded and the expression profile of the different markers is placed next to the cells. A gray arrow indicates the temporal transition along the differentiation path. (**B**) The model of cell-fate acquisition in the neuromast, combining the temporal hierarchy of gene expression relative to the areas of high (purple) or low (pink) Notch activity. (**C**) The temporal transition of hair cells from the division of their progenitor, through the planar inversions indicated by two curved gray arrows on the second scheme from the left, and the eventual realignment of polarized hair cells, shown by the red dots that represent the kinocilia. Two small gray arrows show the centrifugal movement of mature hair cells in the right-most schematic, which propagates planar polarity across the epithelium.

Centrifugal hair-cell movement propagates planar polarity horizontally

Although hair-cell regeneration remains strongly anisotropic, the macula eventually expands symmetrically. This could be due to the development of UHCPs outside the polar compartments during Phases II and III. Alternatively, polar compartments may themselves relocate or expand around the entire neuromast. Although these situations are possible, the weight of the evidence is against them. First, the majority of UHCPs develop within the dorsal or ventral aspect of neuromasts in all three phases of regeneration, and the small percentage of UHCPs that could not be unambiguously located within these compartments would be insufficient to account for the rapid and widespread symmetric expansion of planar polarity. Second, we observed that peripheral hair cells were negative for Atoh1a, indicating that they are older that those located centrally or nearby the polar compartments. Therefore, we conclude that planar polarity is likely to propagate symmetrically because hair cells move away from the midline towards the periphery of the neuromast. It follows that the hair cells located peripherally along a line perpendicular to that of regeneration should be the oldest. Our results on DiASP incorporation support this conclusion.

Planar cell inversions

Live imaging demonstrates that oriented progenitor divisions are not essential for regeneration anisotropy. In addition, we observed that the majority of hair-cell sibling rotate around their contact point immediately after UHCP cytokinesis. To the best of our knowledge, our data is the first description of ‘planar cell

inversions'. This remarkable cellular behavior could offer further mechanistic insights into the process that sustains bilateral symmetry during regeneration. It may reveal a general process that links epithelial polarity to external mechanical cues (Aigouy et al., 2010). It could also play a role in maintaining cellular orientation in plastic tissues with high cellular turnover, such as in the mammalian kidney, lung or brain ventricles (Fischer et al., 2006; Mirzadeh et al., 2010; Saburi et al., 2008; Yates et al., 2010).

Conclusion

In this study we employed transgenic sensors and markers of hair-cell progenitors, combined with high-resolution long-term in toto continuous live imaging, to demonstrate that hair-cell regeneration is strongly anisotropic, and that regeneration anisotropy is regulated by Notch signaling. The model that emerges from our results (summarized in Fig. 6) suggests that bilateral symmetry is sustained by compartmentalized Notch activity, which governs regeneration anisotropy by permitting the stabilization of UHCP identity in the polar compartments. There are several examples of dynamic or stable compartments that allow cells to loose stemness and progress through a differentiation program (Mathur et al., 2010; Voog et al., 2008). In the specific case of the lateral line, the polar compartments appear to oppose a niche by allowing supporting cells to become UHCPs. Further molecular dissection of this process in the zebrafish lateral line may provide deeper insights into the mechanisms that control the homeostasis of tissue architecture.

Acknowledgements

We thank V. Korzh, M. Parsons, N. Lawson, M. Allende, S. Burgess, R. Tsien and T. Whitfield for reagents, and many colleagues for comments on the manuscript. This work was supported by an European Research Council Starting Grant to H.L.-S., the Ministry of Science and Innovation of Spain to H.L.-S., the CRG, and the FCT of Portugal through the GABBA PhD program to F.P.-T.

Author contributions

H.L.-S. designed the project. I.W. and F.P.-T. performed all the experiments. H.L.-S., I.W. and F.P.-T. analyzed the data and wrote the paper. C.S. and S.H. generated the *Tg[Atoh1:TdTomato]* transgenic line.

Competing interests statement

The authors declare no competing financial interests.

Supplementary material

Supplementary material for this article is available at
http://dev.biologists.org/lookup/suppl/doi:10.1242/dev.060566/-/DC1

References

Aigouy, B., Farhadifar, R., Staple, D. B., Sagner, A., Roper, J. C., Jülicher, F. and Eaton, S. (2010). Cell flow reorients the axis of planar polarity in the wing epithelium of *Drosophila*. *Cell* **142**, 773-786.

Axelrod, J. D. (2009). Progress and challenges in understanding planar cell polarity signaling. *Semin. Cell Dev. Biol.* **20**, 964-971.

Baena-López, L. A., Baonza, A. and García-Bellido, A. (2005). The orientation of cell divisions determines the shape of *Drosophila* organs. *Curr. Biol.* **15**, 1640-1644.

Brignull, H. R., Raible, D. W. and Stone, J. S. (2009). Feathers and fins: non-mammalian models for hair cell regeneration. *Brain Res.* **1277**, 12-23.

Chezar, H. H. (1930). Studies on the lateral-line system of amphibia. II. Comparative cytology and innervation of the lateral-line organs in the Urodela. *J. Comp. Neurol.* **50**, 159-175.

Collado, M. S., Burns, J. C., Hu, Z. and Corwin, J. T. (2008). Recent advances in hair cell regeneration research. *Curr. Opin. Otolaryngol. Head Neck Surg.* **16**, 465-471.

Corwin, J. T. and Cotanche, D. A. (1988). Regeneration of sensory hair cells after acoustic trauma. *Science* **240**, 1772-1774.

Daudet, N., Gibson, R., Shang, J., Bernard, A., Lewis, J. and Stone, J. (2009). Notch regulation of progenitor cell behavior in quiescent and regenerating auditory epithelium of mature birds. *Dev. Biol.* **326**, 86-100.

Eddison, M., Le Roux, I. and Lewis, J. (2000). Notch signaling in the development of the inner ear: lessons from *Drosophila*. *Proc. Natl. Acad. Sci. USA* **97**, 11692-11699.

Faucherre, A., Pujol-Martí, J., Kawakami, K. and López-Schier, H. (2009). Afferent neurons of the zebrafish lateral line are strict selectors of hair-cell orientation. *PLoS One* **4**, e4477.

Fischer, E., Legue, E., Doyen, A., Nato, F., Nicolas, J. F., Torres, V., Yaniv, M. and Pontoglio, M. (2006). Defective planar cell polarity in polycystic kidney disease. *Nat. Genet.* **38**, 21-23.

Ghysen, A. and Dambly-Chaudière, C. (2007). The lateral line microcosmos. *Genes Dev.* **21**, 2118-2130.

Go, W., Bessarab, D. and Korzh, V. (2010). atp2b1a regulates Ca(2+) export during differentiation and regeneration of mechanosensory hair cells in zebrafish. *Cell Calcium* **48**, 302-313.

Haas, P. and Gilmour, D. (2006). Chemokine signaling mediates self-organizing tissue migration in the zebrafish lateral line. *Dev. Cell* **10**, 673-680.

Haddon, C., Jiang, Y. J., Smithers, L. and Lewis, J. (1998). Delta-Notch signalling and the patterning of sensory cell differentiation in the zebrafish ear: evidence from the mind bomb mutant. *Development* **125**, 4637-4644.

Hernández, P. P., Olivari, F. A., Sarrazín, A. F., Sandoval, P. C. and Allende, M. L. (2007). Regeneration in zebrafish lateral line neuromasts: expression of the neural progenitor cell marker sox2 and proliferation-dependent and-independent mechanisms of hair cell renewal. *Dev. Neurobiol.* **67**, 637-654.

Hudspeth, A. J. (1985). The cellular basis of hearing: the biophysics of hair cells. *Science* **230**, 745-752.

Itoh, M. and Chitnis, A. B. (2001). Expression of proneural and neurogenic genes in the zebrafish lateral line primordium correlates with selection of hair cell fate in neuromasts. *Mech. Dev.* **102**, 263-266.

Lanford, P. J., Lan, Y., Jiang, R., Lindsell, C., Weinmaster, G., Gridley, T. and Kelley, M. W. (1999). Notch signalling pathway mediates hair cell development in mammalian cochlea. *Nat. Genet.* **21**, 289-292.

Lecuit, T. and Le Goff, L. (2007). Orchestrating size and shape during morphogenesis. *Nature* **450**, 189-192.

Lewis, J. and Davies, A. (2002). Planar cell polarity in the inner ear: how do hair cells acquire their oriented structure? *J. Neurobiol.* **53**, 190-201.

López-Schier, H. (2004). Regeneration: did you hear the news? *Curr. Biol.* **14**, R127-R128.

López-Schier, H. and Hudspeth, A. J. (2006). A two-step mechanism underlies the planar polarization of regenerating sensory hair cells. *Proc. Natl. Acad. Sci. USA* **103**, 18615-18620.

Ma, E. Y., Rubel, E. W. and Raible, D. W. (2008). Notch signaling regulates the extent of hair cell regeneration in the zebrafish lateral line. *J. Neurosci.* **28**, 2261-2273.

Mathur, D., Bost, A., Driver, I. and Ohlstein, B. (2010). A transient niche regulates the specification of *Drosophila* intestinal stem cells. *Science* **327**, 210-213.

Millimaki, B. B., Sweet, E. M. and Riley, B. B. (2010). Sox2 is required for maintenance and regeneration, but not initial development, of hair cells in the zebrafish inner ear. *Dev. Biol.* **338**, 262-269.

Mirzadeh, Z., Han, Y. G., Soriano-Navarro, M., García-Verdugo, J. M. and Álvarez-Buylla, A. (2010). Cilia organize ependymal planar polarity. *J. Neurosci.* **30**, 2600-2610.

Murphey, R. D., Stern, H. M., Straub, C. T. and Zon, L. I. (2006). A chemical genetic screen for cell cycle inhibitors in zebrafish embryos. *Chem. Biol. Drug Des.* **68**, 213-219.

Parinov, S., Kondrichin, I., Korzh, V. and Emelyanov, A. (2004). Tol2 transposon-mediated enhancer trap to identify developmentally regulated zebrafish genes *in vivo*. *Dev. Dyn.* **231**, 449-459.

Parsons, M. J., Pisharath, H., Yusuff, S., Moore, J. C., Siekmann, A. F., Lawson, N. and Leach, S. D. (2009). Notch-responsive cells initiate the secondary transition in larval zebrafish pancreas. *Mech. Dev.* **126**, 898-912.

Rida, P. C. and Chen, P. (2009). Line up and listen: Planar cell polarity regulation in the mammalian inner ear. *Semin. Cell Dev. Biol.* **20**, 978-985.

Ryals, B. M. and Rubel, E. W. (1988). Hair cell regeneration after acoustic trauma in adult Coturnix quail. *Science* **240**, 1774-1776.

Saburi, S., Hester, I., Fischer, E., Pontoglio, M., Eremina, V., Gessler, M., Quaggin, S. E., Harrison, R., Mount, R. and McNeill, H. (2008). Loss of Fat4 disrupts PCP signaling and oriented cell division and leads to cystic kidney disease. *Nat. Genet.* **40**, 1010-1015.

Strutt, H. and Strutt, D. (2009). Asymmetric localisation of planar polarity proteins: Mechanisms and consequences. *Semin. Cell Dev. Biol.* **20**, 957-963.

Villablanca, E. J., Renucci, A., Sapède, D., Lec, V., Soubiran, F., Sandoval, P. C., Dambly-Chaudière, C., Ghysen, A. and Allende, M. L. (2006). Control of cell migration in the zebrafish lateral line: implication of the gene "tumour-associated calcium signal transducer," tacstd. *Dev. Dyn.* **235**, 1578-1588.

Voog, J., D'Alterio, C. and Jones, D. L. (2008). Multipotent somatic stem cells contribute to the stem cell niche in the *Drosophila* testis. *Nature* **454**, 1132-1136.

Williams, J. A. and Holder, N. (2000). Cell turnover in neuromasts of zebrafish larvae. *Hear. Res.* **143**, 171-181.

Wodarz, A. and Nathke, I. (2007). Cell polarity in development and cancer. *Nat. Cell Biol.* **9**, 1016-1024.

Yates, L. L., Schnatwinkel, C., Murdoch, J. N., Bogani, D., Formstone, C. J., Townsend, S., Greenfield, A., Niswander, L. A. and Dean, C. H. (2010). The PCP genes Celsr1 and Vangl2 are required for normal lung branching morphogenesis. *Hum. Mol. Genet.* **19**, 2251-2267.

Zallen, J. A. (2007). Planar polarity and tissue morphogenesis. *Cell* **129**, 1051-1063.